

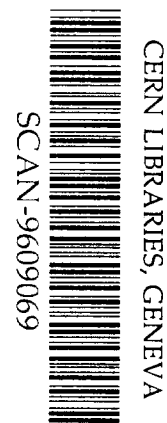
UNIVERSITY OF OXFORD

Department of Physics

PARTICLE AND NUCLEAR PHYSICS

CLUSTER KNOCKOUT NUCLEAR REACTIONS
AND MOMENTUM DISTRIBUTIONS OF
CLUSTERS IN ATOMIC NUCLEI

K. Spasova, A.N. Antonov and P.E. Hodgson

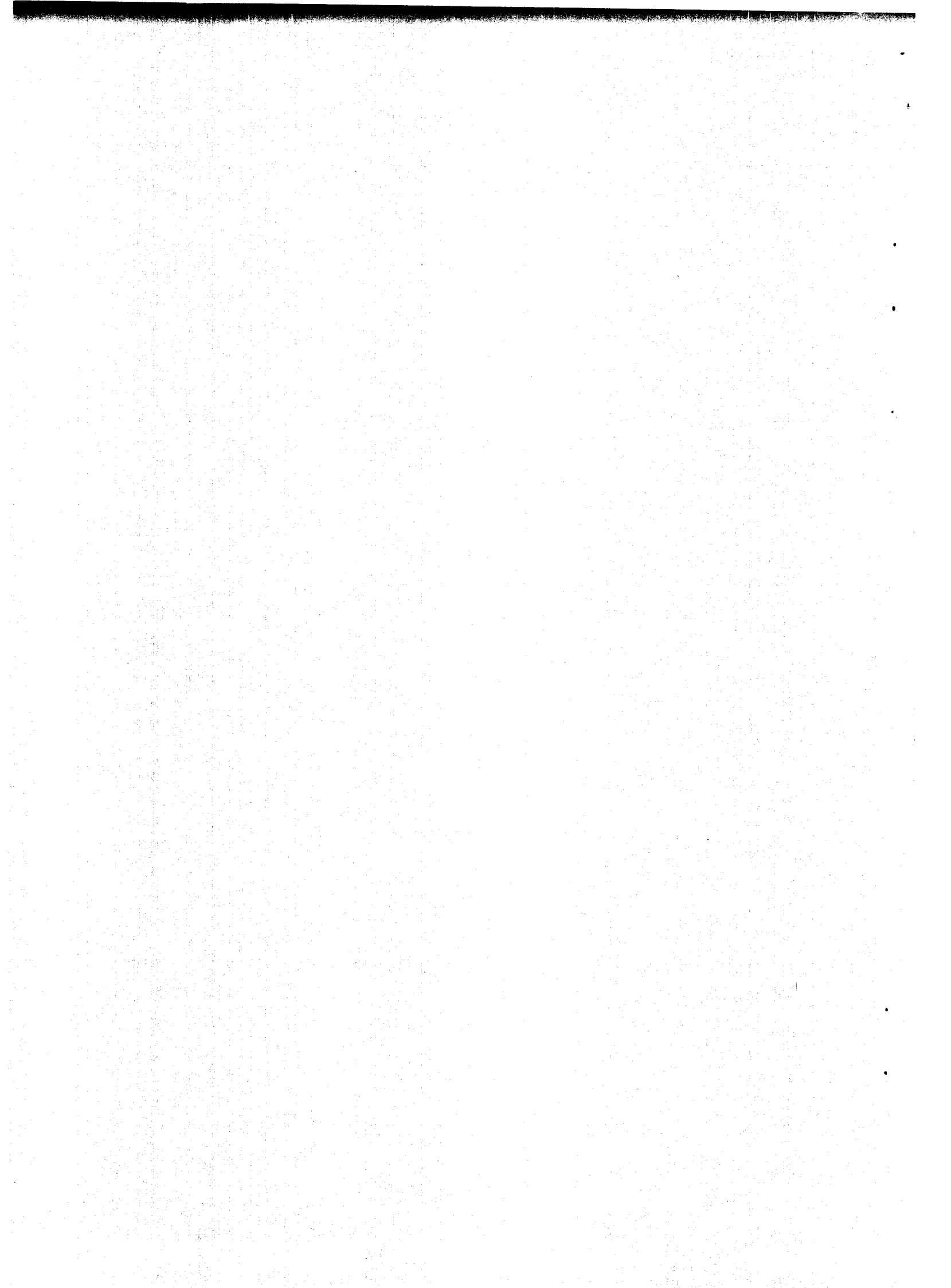


sw9638

To be published in the *Bulgarian Journal of Physics*
Volume 23, No. 3-4, 1996

Ref: OUNP-96-13

Address: Department of Physics
Particle & Nuclear Physics
Keble Road
Oxford OX1 3RH
U.K.



CLUSTER KNOCKOUT NUCLEAR REACTIONS AND MOMENTUM
DISTRIBUTIONS OF CLUSTERS IN ATOMIC NUCLEI

K. Spasova, A. N. Antonov and P. E. Hodgson

Abstract

The momentum distributions of deuteron- and alpha-clusters obtained in theoretical correlation methods are fitted in calculations of the cross-sections of deuteron- and alpha-knockout reactions with electrons. It is shown that the predictions for the momentum distributions at low momenta ($0 \leq k \leq 0.3 \text{ fm}^{-1}$) are in a qualitative agreement with the cluster momentum distributions found to give the best fit of the experimental data for the cross-sections of the ${}^6\text{Li}(e, e'd)$ and ${}^6\text{Li}(e, e'\alpha)$ reactions and with other calculations.

CLUSTER KNOCKOUT NUCLEAR REACTIONS AND MOMENTUM
DISTRIBUTIONS OF CLUSTERS IN ATOMIC NUCLEI⁺

K. Spasova⁽¹⁾, A. N. Antonov^(1, 2) and P. E. Hodgson⁽³⁾

⁽¹⁾ University of Shumen, Shumen 9700, Bulgaria

⁽²⁾ Institute of Nuclear Research and Nuclear Energy,
Bulgarian Academy of Sciences, Sofia 1784, Bulgaria

⁽³⁾ Nuclear Physics Laboratory, Department of Physics,
University of Oxford, Oxford OX1-3RH, U.K.

I. Introduction

Many aspects of nuclear structure and reactions suggest that nucleons can combine to form transient sub-structures or clusters, and among these the alpha-particle is the most likely for reasons of energy and symmetry [1]. It is important to determine the degree of the clustering not only to facilitate an economical description of nuclear structure and reactions, but also to learn more about the nucleon-nucleon correlations in the nuclear interior.

The character of the clustering in atomic nuclei depends on the nuclear size. Light nuclei can be considered to consist of linked clusters of alpha-particles, deuterons and nucleons. In heavier nuclei alpha-clusters can be expected in the region of the nuclear surface since condensation into alpha-clusters is energetically favourable at densities around one-third of that in the nuclear interior [2]. Many nuclei decay spontaneously by emitting alpha-clusters and heavy fragments. Fusion reactions are affected

⁺This work is partially supported by the Agreement between the Bulgarian Academy of Sciences and the Royal Society and by the Bulgarian National Science Foundation under Contracts No. Phi-406 and Phi-527.

by clustering in intermediate states and breakup reactions provide evidence of cluster structure in the projectile. At higher energies some nuclear reactions preferentially proceed by cluster transfer or by knockout and pickup reactions. At very high energies nuclei can be fragmented into a wide range of clusters of nucleons.

In the early studies of the alpha clustering in nuclei, knockout reactions such as $(p, p\alpha)$ [3,4] and $(\alpha, 2\alpha)$ [5,6,7,8,9] have been considered. The interpretation of their cross-sections is, however, complicated due to the nuclear and Coulomb distortions in the incident and outgoing channels. On the other hand, the use of electron beams has the advantage that the nuclear distortion is absent and the Coulomb distortion reduced. For these reasons reactions such as $(e, e'd)$ and $(e, e'\alpha)$ [10,11,12,13,14] are now more intensively used though their cross-sections are much smaller compared with those of the other knockout reactions mentioned above.

In the theoretical analyses of the $(p, p\alpha)$ and $(\alpha, 2\alpha)$ cross-sections the plane wave impulse approximation (PWIA) [3,6,7] or the distorted wave impulse approximation (DWIA) [4,7,9] have been used. In the PWIA the reaction cross-section depends on the momentum distribution of the alpha-cluster in the target nucleus. The DWIA analyses give the cross-sections in terms of the "distorted momentum distribution" of the cluster. The DWIA calculations of (p, α) reactions at 72 MeV show that the analysing power in the continuum can be reproduced by the α -particle knockout mechanism but not by the pickup mechanism [15]. The angular distribution of the (α, α') reaction can also be described by taking into account the interaction of the incoming α -particle with preformed α -particles in the target nucleus [16]. Thus including the cluster motion in the target nucleus allows a better description of all these reactions.

The importance of the α -particle momentum distribution (AMD) has been discussed in [17,18]. It is an essential component

of the calculations of the cross-sections and provides a sensitive probe of the short-range nucleon-nucleon correlations in nuclei. The latter are responsible for the high-momentum components of the nucleon and cluster momentum distributions which are obtained from experimental data on different features of nuclear reactions and can be described by theoretical models going beyond the mean-field approximation (e.g. [18-21]).

The aim of the present work is to test the momentum distributions of deuteron- and alpha-clusters obtained in correlation theoretical methods in analyses of deuteron- and alpha-knockout reactions with electrons. Though the available experimental data are quite limited and only the low-momentum behaviour of the cluster momentum distributions can be tested, we hope that such an analysis will be a prelude to the more extensive studies of cluster correlations in nuclei.

In Section 2 we present the theoretical scheme for the calculations of the cluster knockout reactions cross-section. Section 3 is devoted to the theoretical calculations of alpha- and deuteron-cluster momentum distributions within some theoretical correlation methods. The results of the calculations and the discussion are given in Section 4.

2. Cross-sections of cluster-knockout reactions with electrons.

In this paper we discuss $(e, e'x)$ reactions, where x is a composite particle, namely a deuteron or an alpha-particle.

The cross-section for ${}^6\text{Li}(e, e'\alpha)$ reaction is calculated and analysed in [10]. The empirical data for the $(e, e'd)$ reaction on various nuclei are given, for instance, in [10, 22]. The light nucleus ${}^6\text{Li}$ has a high level of clustering. Detection of the deuteron and the α -particle allows a symmetric investigation of clusterization in this nucleus.

The kinematics of the $(e, e'x)$ process is shown in the Fig.1.

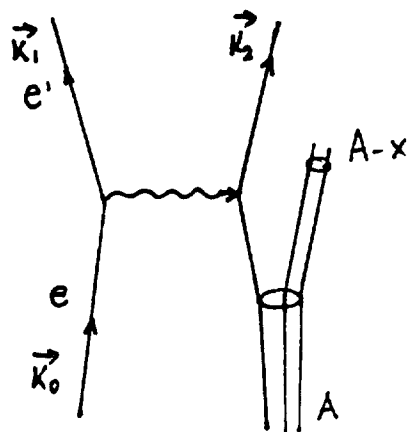


Fig. 1. The kinematics of the process $(e, e'x)$.

The basic relations are:

$$\begin{aligned}
 T_0 &= T_1 + T_2 + T_r + S, \\
 k_0 &= k_1 + k_2 + k_r, \\
 k_r &= -k_3, \\
 q &= k_0 - k_1,
 \end{aligned}
 \tag{1}$$

where k_0, T_0, k_1, T_1 and k_2, T_2 are the momenta and kinetic energies of the incident and the outgoing electron and of the emitted fragment, respectively, k_r is the momentum of the residual nucleus and S is the missing energy.

Following [10], the cross-section of the $(e, e'\alpha)$ and $(e, e'd)$ reactions can be written in the form:

$$\frac{d^3\sigma}{dT_1 d\Omega_1 d\Omega_2} = C(x) \left(\frac{d\sigma}{d\Omega_1} \right)_{e-x} |G(k_3)|^2 P_x, \tag{2}$$

where $|G(k_3)|^2$ is the momentum distribution of the x -cluster and P_x is the probability of finding it in the initial nucleus. In eq. (2)

$$C(x) = \frac{T_0}{T_1} \frac{M_x M_{A-x} |k_2|^3}{|k_2|^2 \cdot (M_x + M_{A-x}) - M_x \cdot |k_2| \cdot |q| \cdot \cos x}, \tag{3}$$

where M_x and M_{A-x} are the masses of the cluster and the residual nucleus, respectively, and x is the angle between the momenta q and k_2 ($k_2 \cdot q = |k_2| \cdot |q| \cos x$).

The normalization of the momentum distribution is [23]:

$$(2\pi)^{-3} \int |G(k_3)|^2 d^3k_3 = 1. \tag{4}$$

The cross-section for the electron elastic scattering on the α -particle is given in [23]:

$$\left(\frac{d\sigma}{d\Omega_1} \right)_{e-\alpha} = \sigma_{\text{Mott}} \cdot F^2(q), \tag{5}$$

where $F(q)$ is the form factor of the nucleus and σ_{Mott} is the Mott cross-section.

The cross-section of the electron elastic scattering from deuterons is given in [24]:

$$\left(\frac{d\sigma}{d\Omega}\right)_{e-d} = \sigma_{\text{Mott}} \left\{ 1 + \frac{2T_0}{M_d} \sin^2(\vartheta/2) \right\} \left\{ G_0^2 + G_2^2 + \left[1 + 2 \left(1 - \frac{q^2}{4M_d^2} \right) \right. \right. \\ \left. \left. \tan^2(\vartheta/2) \right] G_m^2 \right\} , \quad (6)$$

where G_0, G_2 and G_m are the electric, the quadrupole and the magnetic form factors, respectively, and ϑ is the angle between the momenta k_0 and k_1 .

3. Cluster Momentum Distributions.

As mentioned above, the cluster momentum distributions are important for the understanding of the reactions with cluster knockout, such as $(e, e'\alpha)$, $(\alpha, 2\alpha)$, $(e, e'd)$ and other reactions. In this section we present briefly some methods for calculating the deuteron- and α -particle momentum distributions in nuclei.

3.1. The two-nucleon momentum distribution.

The two-nucleon momentum distribution (TNMD) $n^{(2)}(\xi_1, \xi_2)$ is defined using the diagonal elements of the two-body density matrix [18]:

$$\rho^{(2)}(\xi_1, \xi_2; \xi_1, \xi_2) = (1/2)A(A-1) \sum \int dr_3 \dots dr_A \Psi^*(\xi_1, \xi_2, \xi_3, \dots, \xi_A) \times \\ \Psi(\xi_1, \xi_2, \xi_3, \dots, \xi_A) , \quad (7)$$

where $\Psi(\{\xi_i\})$ ($i=1, \dots, A$) is the normalized total wave function of a system of A nucleons. Each coordinate ξ_i is a combination of a space (r_i), spin (σ_i) and isospin (τ_i) coordinates: $\xi_i = (r_i; \tau_i, \sigma_i) = (r_i; \eta_i)$. In the momentum space ($\xi_i = (k_i; \tau_i, \sigma_i)$) the momentum

distribution has the form:

$$n^{(2)}(\xi_1, \xi_2) = \rho^{(2)}(\xi_1, \xi_2; \xi_1, \xi_2) \quad (8)$$

Using the general relationship (8) one can introduce the centre-of-mass $n^{(cm)}$ and relative $n^{(rel)}$ TNMD [18,25]. These quantities have been studied by different theoretical methods, such as the phenomenological one of Haneishi and Fujita [25], the ATMS correlation method of Akaishi [26] for the ${}^4\text{He}$ nucleus and in the coherent density fluctuation model (CDFM) [27,18] and in the generator coordinate method (GCM) [28,18] for the ${}^4\text{He}$, ${}^{16}\text{O}$ and ${}^{40}\text{Ca}$ nuclei.

In the ATMS correlation method [26] the obtained TNMD $n^{(cm)}$ and $n^{(rel)}$ are parametrized by

$$n^{(cm)(rel)} = N(\exp(-p^2/(2a)) + s \exp(-p^2/(2at))) \quad (9)$$

with $\{a(\text{fm}^{-2}), s, t\} = \{0.42 \times 3, 0.01, 8\}$ for $n^{(cm)}$ and $\{0.42/4, 0.015, 6\}$ for $n^{(rel)}$. It is pointed out that the TNMD have prominent high-momentum components which reflect the role of the nucleon-nucleon correlations.

The coherent density fluctuation model (CDFM) [18,19,21] has been extended in [27] to calculate the TNMD $n^{(cm)}$ and $n^{(rel)}$. The wave function Ψ is considered in the form:

$$\Psi(\xi_1, \dots, \xi_A) = \int f(x) \varphi(x; \xi_1, \dots, \xi_A) dx, \quad (10)$$

where the generating function $\varphi(x; \xi_1, \dots, \xi_A)$ describes the state of A - nucleons in a sphere with radius x . In the case of nuclei with $Z=N=A/2$ the p-n centre-of mass and relative motion TNMD normalized to $A/4$ have the form [27,18]:

$$n_{np}^{(cm)}(p) = A \int_0^{\infty} dx |f(x)|^2 \Omega(x) \left[1 - \frac{3|p|}{4k_F(x)} + \frac{1}{16} \frac{|p|^3}{k_F^3(x)} \right] \times \theta(k_F(x) - |p|/2), \quad (11)$$

$$n_{np}^{(rel)}(q) = 8A \int_0^{\infty} dx |f(x)|^2 \Omega(x) \left[1 - \frac{3|q|}{2k_F(x)} + \frac{1}{2} \frac{|q|^3}{k_F^3(x)} \right] \times \theta(k_F(x) - |q|), \quad (12)$$

where the weight function $|f(x)|^2$ is:

$$|f(x)|^2 = -\frac{1}{\rho(x)} \frac{d\rho(r)}{dr} \Big|_{r=x}, \quad \rho_0(x) = \frac{3A}{4\pi x^3} \quad (13)$$

in the case of monotonically-decreasing density distribution ($d\rho/dr \leq 0$) and $\Omega(x) = \frac{4}{3}\pi x^3$.

In the GCM the TNMD has the following form for the case of n-p pairs and $Z=N$ nuclei:

$$n_{np}^{(2)}(k_1, k_2) = \frac{1}{4} \int dx f^*(x) \int dx' f(x') I(x, x') \tilde{\rho}(x, x'; k_1) \times \tilde{\rho}(x, x'; k_2), \quad (14)$$

where

$$\tilde{\rho}(x, x'; k) = \sum_{\lambda, \mu=1}^{A/4} (N^{-1})_{\mu\lambda} \tilde{X}_{\lambda}^*(x, k) \tilde{X}_{\mu}(x', k), \quad (15)$$

$\tilde{X}_{\lambda}(x, k)$ being the Fourier transform of the single-particle orbital $X_{\lambda}(x, r)$ and each orbital state is occupied by four nucleons. The function $f(x)$ in (14) and (15) is the solution of the Hill-Wheeler-Griffin equation and $I(x, x')$ is the overlap kernel within the GCM [19].

3.2. The α -particle momentum distribution.

The alpha-particle momentum distribution has been calculated

in the framework of the CDFM [17,18]. The definition of the four-body density matrix has the form

$$\rho^{(4)}(\xi_1, \xi_2, \xi_3, \xi_4; \xi'_1, \xi'_2, \xi'_3, \xi'_4) = \frac{A(A-1)(A-2)(A-3)}{4!} \sum_{q_5, \dots, q_A} \int dr_5 \dots dr_A \Psi^+(\xi_1, \xi_2, \xi_3, \xi_4, \xi_5, \dots, \xi_A) \Psi(\xi'_1, \xi'_2, \xi'_3, \xi'_4, \xi_5, \dots, \xi_A). \quad (16)$$

In the CDFM the many-body wave function has the GCM-form:

$$\psi(\xi_1, \xi_2, \xi_3, \dots, \xi_A) = \int dx |f(x)|^2 \Phi(x; \xi_1, \xi_2, \dots, \xi_A), \quad (17)$$

where Φ is a Slater determinant wave function built up from plane waves in a volume $V(x) = \frac{4}{3}\pi x^3$ and $|f(x)|^2$ is given by eq.(13).

The four-body momentum distribution $n^{(4)}(\xi_1, \xi_2, \xi_3, \xi_4)$ can be expressed by the diagonal elements of the four-body matrix in momentum space

$$n^{(4)}(\xi_1, \xi_2, \xi_3, \xi_4) = \rho^{(4)}(\xi_1, \xi_2, \xi_3, \xi_4; \xi_1, \xi_2, \xi_3, \xi_4). \quad (18)$$

The alpha-particle momentum distribution in the CDFM has the following final form [17,18]:

$$n^{(\alpha)}(k_1, k_2, k_3, k_4) = \int dx |f(x)|^2 V^4(x) \prod_{i=1}^4 \delta(k_i f(x) - |k_i|) \quad (19)$$

with the normalization:

$$\frac{1}{(2\pi)^{12}} \int \prod_{i=1}^4 dk_i n^{(\alpha)}(k_1, k_2, k_3, k_4) = (A/4)^4. \quad (20)$$

The explicit form of the centre-of-mass α -particle momentum distribution is:

$$n_{cm}^{\alpha}(P) = (A/4)^4 (2\pi)^{-12} \int d\Omega_p \int dp_1 \int dp_2 \int dp_3 \times \int_0^a dx |f(x)|^2 \left(\frac{4}{3}\pi x^3\right)^4, \quad (21)$$

with $a = \alpha / \max \{S_1, S_2, S_3, S_4\}$, where $\max \{S_1, S_2, S_3, S_4\}$ is the largest of the quantities

$$\begin{aligned} S_1 &\equiv \left| \frac{1}{4}P + p_1 + \frac{1}{2}p_2 + \frac{1}{3}p_3 \right|, \\ S_2 &\equiv \left| \frac{1}{4}P - p_1 + \frac{1}{2}p_2 + \frac{1}{3}p_3 \right|, \\ S_3 &\equiv \left| \frac{1}{4}P - \frac{1}{2}p_2 + \frac{1}{3}p_3 \right|, \\ S_4 &\equiv \left| \frac{1}{4}P - p_3 \right|, \\ \alpha &\equiv (9\pi A/8)^{1/3} \end{aligned} \quad (22)$$

and P, p_1, p_2, p_3 are the Jacobi momenta [29].

The c.m. AMD (21) is with the normalization condition:

$$\int n_{cm}^{\alpha}(P) P^2 dP = 1. \quad (24)$$

The results for n_{cm}^{α} calculated for the ${}^9\text{Be}$, ${}^{12}\text{C}$, ${}^{16}\text{O}$, ${}^{20}\text{Ne}$, ${}^{24}\text{Mg}$, ${}^{28}\text{Si}$, ${}^{32}\text{S}$, and ${}^{40}\text{Ca}$ nuclei were obtained in [17,18].

4. Results and discussion.

In this Section we test the cluster momentum distributions described in Sect.3 in calculations of cross-sections of cluster knockout reactions. It should be noted that the possibilities of comparing theoretical calculations of $(e, e'\alpha)$ and $(e, e'd)$ -reaction cross-sections using α - and d -momentum distributions, respectively, with the empirical data are limited. The reason is that the available experimental results are scarce, they are mainly qualitative and can test the cluster momentum distributions only for low momenta ($0 < p < 1 \text{ fm}^{-1}$). Nevertheless, though N - N correlation effects are reflected mainly in the behaviour of the cluster momentum distribution at higher momenta ($p \geq 2 \text{ fm}^{-1}$), it is of interest to compare the theoretical

results with the existing data which are related to the low momentum components of the cluster momentum distributions.

In this work we analyze firstly the $(e, e'\alpha)$ cross-section (using the expressions (2) and (3)) and the α -cluster momentum distribution $n^{(\alpha)}$ (Eq.(21)) obtained in [17]. As can be seen from the normalizations (Eqs.(4) and (24)) the relationship between the two momentum distributions is:

$$n^{(\alpha)}(k_3) = \frac{|G(k_3)|^2}{2\pi^2} \quad (25)$$

Here we note that in [17] the $n^{(\alpha)}$ are obtained for the ${}^9\text{Be}$, ${}^{12}\text{C}$, ${}^{16}\text{O}$, ${}^{20}\text{Ne}$, ${}^{24}\text{Mg}$, ${}^{28}\text{Si}$, ${}^{32}\text{S}$, ${}^{40}\text{Ca}$ nuclei, but not for the case of the ${}^6\text{Li}$ nucleus. On the other hand, the α -cluster momentum distributions in the considered cases are quite similar numerically. We therefore can only test the α -cluster momentum distribution $n^{(\alpha)}$ calculated for ${}^9\text{Be}$ in the case of ${}^6\text{Li}$. For this purpose we determine by calculations of the ${}^6\text{Li}(e, e'\alpha)$ cross-section the α -cluster momentum distribution that fits the experimental data in the best way. In Fig.2 the calculated ${}^6\text{Li}(e, e'\alpha)$ cross-section (dashed line) is compared with the experimental data and the calculations from [10]. In Fig.3 we present the α -cluster momentum distribution (solid line) that fits the data for the cross-section of the α -knockout on ${}^6\text{Li}$ and compared it with that for ${}^9\text{Be}$ from [17]. The comparison shows that the experimental data make it possible to analyze $n^{(\alpha)}$ at very small momenta, namely in the region between 0.04 fm^{-1} and 0.3 fm^{-1} (this is the reason why the drawn fitted cluster momentum is given only up to 0.3 fm^{-1}). It can be seen also that in this low-momentum region the $n^{(\alpha)}$ for ${}^6\text{Li}$ has to be larger than the calculated $n^{(\alpha)}$ for ${}^9\text{Be}$ in order to fit in the best way the cross-section data for ${}^6\text{Li}(e, e'\alpha)$ -reaction.

We analyze secondly the $(e, e'd)$ cross-section using Eqs.

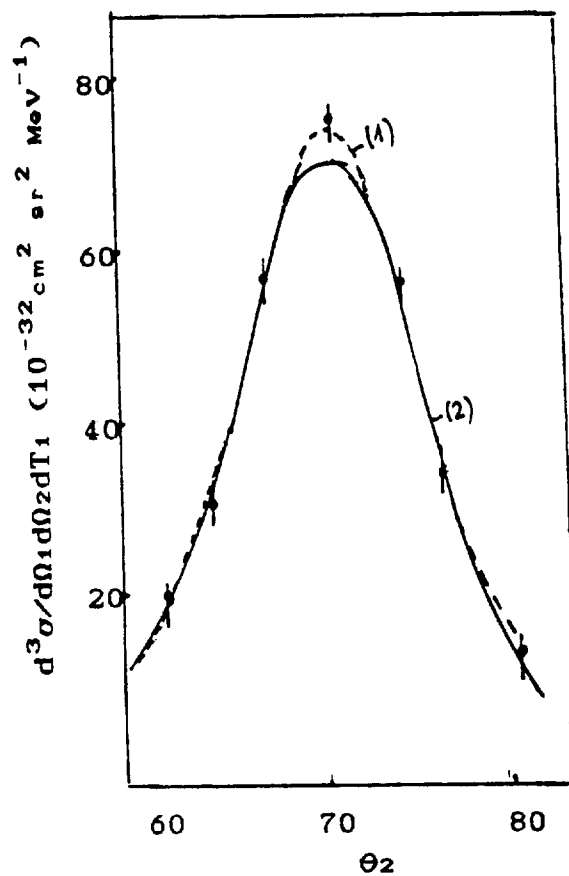


Fig. 2. The cross-section of the ${}^6\text{Li}(e, e'\alpha)$ reaction. The curve (1) is the result of this work obtained by the best fit of $n_{\text{cm}}^{(\alpha)}$ to the experimental data. The experimental data are given by black points from [10].

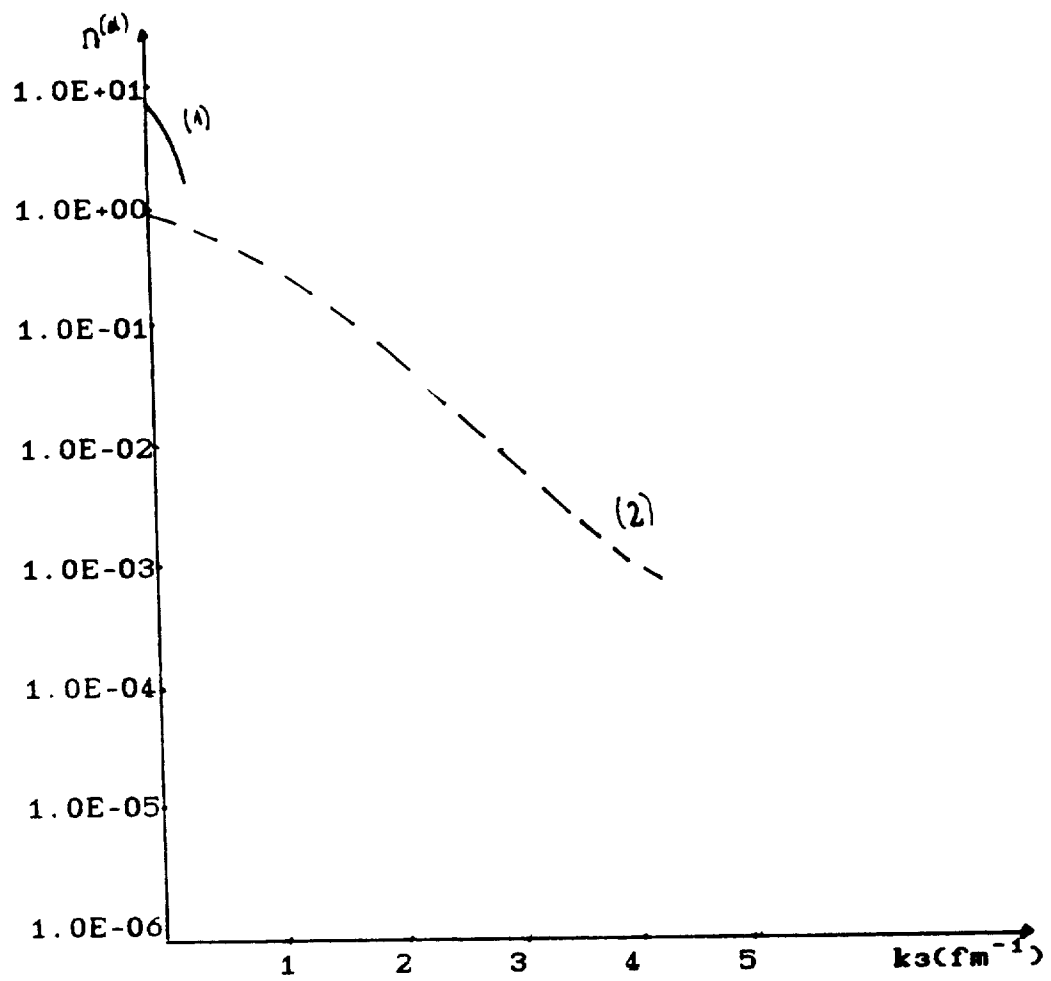


Fig. 3. The alpha-particle momentum distribution used in the calculations (curve 1) and that for ${}^9\text{Be}$ from [17].

(2), (3) and (6). We should like to mention that in this work we use d- cluster momentum distributions obtained in correlation theoretical methods for the ^4He nucleus, but not for ^6Li nucleus. We shall consider particularly distributions which can be tested using the cross-section calculations. The first one is the two-nucleon momentum distributions $n_{np}^{(cm)}(\mathbf{k})$ given by the coherent density fluctuation model (CDFM) (Eq.11) The cross-section can be written in the form:

$$\frac{d^3\sigma}{dT_2 d\Omega_1 d\Omega_2} = \left[\frac{d\sigma}{d\Omega} \right]_{e-d} C(x) \tilde{n}_{np}^{(cm)}(\mathbf{k}), \quad (26)$$

where

$$\tilde{n}_{np}^{(cm)}(\mathbf{k}) = \frac{n_{np}^{(cm)}(\mathbf{k})}{8\pi^3} \quad (27)$$

and the normalization condition is

$$\int n_{np}^{(cm)} d^3(\mathbf{k}) = 1 \quad (28)$$

The second deuteron-cluster momentum distribution is that one ($|G(k_3)|^2$) used in [10].

The relation between the two momentum distributions $\tilde{n}_{np}^{(cm)}(\mathbf{k})$ and $|G(k_3)|^2$ has the form:

$$\tilde{n}_{np}^{(cm)}(\mathbf{k}) = |G(k_3)|^2 \cdot P_d \quad (29)$$

Here we should like to mention that our cluster momentum distributions have been calculated within a density matrix approach, where we do not use an assumption for a cluster already formed in the nucleus. Therefore it is not necessary to introduce an additional factor P_d giving the probability to find the deuteron-like cluster in the nucleus for the cross-section calculations.

Finally, we determine by calculations of the ${}^6\text{Li}(e,e'd)$ cross-section of the d-cluster momentum distribution that fits the experimental data in the best way. The calculated cross-section of the ${}^6\text{Li}$ nuclei using this momentum distribution is given in Fig.4. The comparison of the deuteron-cluster momentum distributions, obtained for ${}^4\text{He}$ in various theoretical approaches with that one which fits the empirical data for the ${}^6\text{Li}(e,e'd)$ reaction is given in Fig.5. It can be seen that the fitted d-cluster MD is close to the predictions for the $n_{np}^{(cm)}(k)$ in ${}^4\text{He}$ in this low-momentum region.

In conclusion the results of the present work can be summarized as follows:

1) Cluster momentum distributions obtained from correlation methods have been used in analyses of the cross-sections of $(e,e'\alpha)$ and $(e,e'd)$ reactions on the ${}^6\text{Li}$ nucleus.

2) It is shown that the available experimental data give information about a limited region of the cluster momentum distributions at quite small values of the momenta ($0 \leq k \leq 0.3\text{fm}^{-1}$).

3) The values of the alpha- and the deuteron- cluster momentum distributions at low momenta which have been determined by the best fit to the experimental data for the ${}^6\text{Li}(e,e'\alpha)$ and ${}^6\text{Li}(e,e'd)$ reaction cross-sections are in a qualitative agreement with the theoretical predictions for the cluster momentum distributions.

Finally, we should like to emphasize that experiments on cluster knockout reactions in which high-momentum components of the cluster momentum distributions (containing information on clusterization correlations in nuclei) can be tested, are highly desirable.

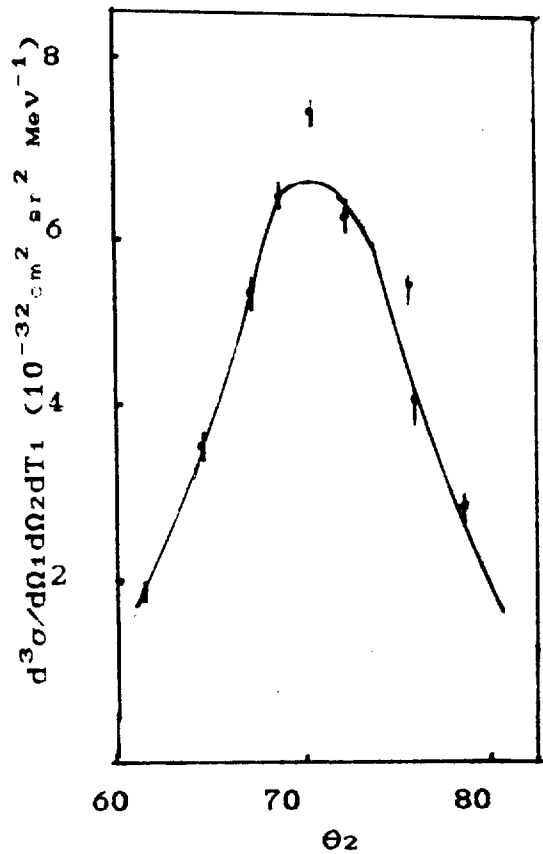


Fig. 4. The cross-section of the ${}^6\text{Li}(e, e'd)$ reaction. The solid curve is the result of this work obtained by the best fit of $n_{np}^{(cm)}$ to the experimental data. The experimental data are given by black points from [10].

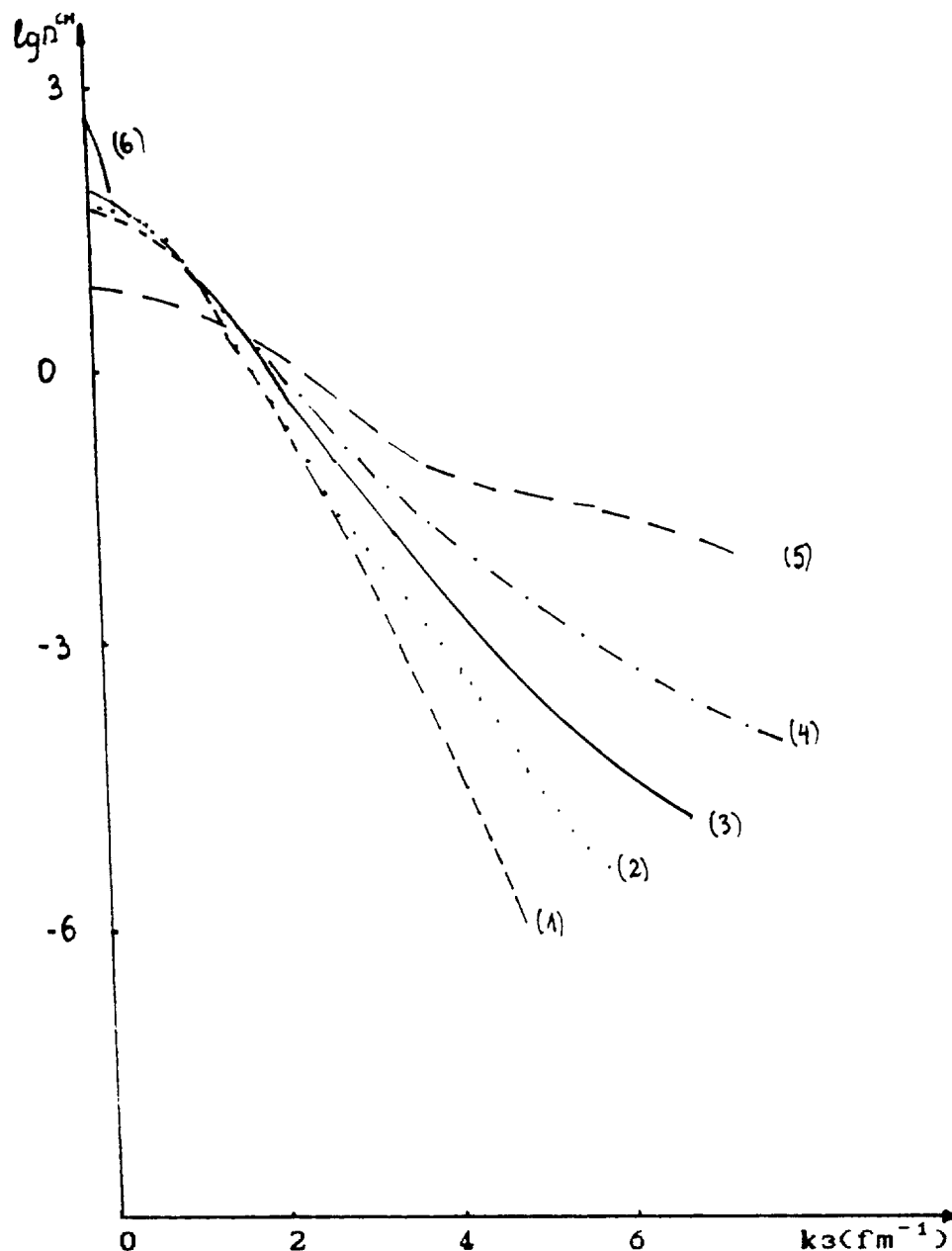


Fig. 5. The two-nucleon centre-of-mass momentum distributions of n-p pairs in ${}^4\text{He}$. The curve (1): phenomenological distribution from [25]; the curve (2): the result of the GCM with harmonic-oscillator construction potential; the curve (3): the result of the GCM with square-well construction potential [28]; the curve (4): the CDFM result [27]; the curve (5): the ATMS result [26]; the curve (6): the $n_{np}^{(cm)}$ momentum distribution which gives the best fit to the data for the ${}^6\text{Li}(e, e'd)$ reaction.

REFERENCES

- [1] P. E. Hodgson: in *Proc. Fifth Int. Conf. Clustering Aspects in Nuclear and Subnuclear Systems*, Kyoto, 1988, *J. Phys. Soc. Jpn.* **58**, Suppl. p. 755 (1989); *Contemporary Physics* **31**, 99 (1990).
- [2] D. Brink and J. J. Castro: *Nucl. Phys.* **A216**, 109 (1973).
- [3] A. N. James, H. G. Pugh: *Nucl. Phys.* **42**, 441 (1963).
- [4] T. A. Garey, P. G. Roos, N. S. Chant, A. Nadasen, H. L. Chen: *Phys. Rev.* **C23**, 576 (1981).
- [5] G. Igo, L. F. Hansen, T. J. Gooding: *Phys. Rev.* **131**, 337 (1963).
- [6] J. W. Watson, H. G. Pugh, P. G. Roos, D. A. Goldberg, R. A. Riddle, D. I. Bonbright: *Nucl. Phys.* **A172**, 513 (1971); M. Jain, P. G. Roos, H. G. Pugh, H. D. Holmgren: *Nucl. Phys.* **A153**, 49 (1970).
- [7] N. Chirapatpimol, J. C. Fong, M. M. Gazzaly, G. Igo, A. D. Liberman, R. J. Ridge, S. L. Verbeck, C. A. Whitten Jr., D. G. Kovar, V. Perez-Mendez, N. S. Chant, P. G. Roos: *Nucl. Phys.* **A264**, 379 (1976).
- [8] W. E. Dollhoph, C. F. Perdrisat, P. Kitching, W. C. Olsen: *Nucl. Phys.* **A316**, 350 (1979).
- [9] C. W. Wang, N. S. Chant, P. G. Roos, A. Nadasen, T. A. Garey: *Phys. Rev.* **C21**, 1705 (1980).
- [10] J. P. Genin, J. Julien, M. Rambaut, C. Samour, A. Palmeri and Vinciguerra: *Phys. Lett.* **52B**, 46 (1974).
- [11] Th. Kihm, K. T. Knöpfle, H. Riedesel, P. Voruganti, H. J. Emrich, G. Fricke, R. Neuhausen, R. K. M. Schneider: *Phys. Rev. Lett.* **56**, 2789 (1986).
- [12] V. F. Dmitriev, D. M. Nikolenko, S. G. Popov, I. A. Rachek, D. K. Toporkov, E. P. Tsentelovich, B. B. Voitserkowski, V. G. Zelevinsky: *Nucl. Phys.* **A464**, 237 (1987).
- [13] I. G. Evseev, V. P. Lichachev, V. L. Agranovich, Yu. V. Vladimirov, S. A. Paschuk, G. A. Savitzkyi, V. B. Shostak: *Ukr. Fiz. Zh.* **35**, 839 (1990).
- [14] H. P. Blok: In *Proc. Fifth Int. Conf. Clustering Aspects in Nuclear and Subnuclear Systems*, Kyoto, 1988, *J. Phys. Soc. Jpn.* **58**, Suppl. p. 409 (1989).

- [15] R. Bonetti, F. Crespi, K. -I. Kubo, *Nucl. Phys.* **A499**, 381 (1989).
- [16] R. Bonetti, R. Colombo, K. -I. Kubo: *Nucl. Phys.* **A420**, 109 (1984).
- [17] A. N. Antonov, E. N. Nikolov, I. Zh. Petkov, P. E. Hodgson, G. A. Lazissis: *Bulg. J. Phys.* **19**, 11 (1992).
- [18] A. N. Antonov, P. E. Hodgson, I. Zh. Petkov: *Nucleon Correlations in Nuclei* (Springer-Verlag, Berlin, 1993).
- [19] A. N. Antonov, P. E. Hodgson, I. Zh. Petkov: *Nucleon Momentum and Density Distributions in Nuclei* (Clarendon Press, Oxford, 1988).
- [20] A. N. Antonov, Chr. V. Christov, I. Zh. Petkov: *Nuovo Cimento*, **A91**, 119 (1986).
- [21] A. N. Antonov, V. A. Nikolaev, I. Zh. Petkov: *Bulg. J. Phys.* **6**, 151 (1979); *Z. Phys.* **A297**, 257 (1980).
- [22] H. P. Blok: *In Proc. 5th Int. Conf. on Nuclear Reaction Mechanisms*, Varenna, Italy, June (1991), ed. by E. Gadioli, Milano p. 428; Preprint EMIN 91-05, Amsterdam (1991).
- [23] T. A. Griffy, R. J. Oakes, H. M. Schwartz, *Nucl. Phys.*, **86**, 313 (1966).
- [24] T. A. Griffy, L. I. Shiff, in: *High Energy Physics*, vol. 1, New York, 1967, p. 341.
- [25] Y. Haneishi, T. Fujita: *Phys. Rev.* **C33**, 260 (1986).
- [26] Y. Akaishi, *Nucl. Phys.* **A416**, 409, (1984).
- [27] A. N. Antonov, I. S. Bonev, Chr. V. Christov, I. Zh. Petkov: *Nuovo Cimento* **A101**, 639 (1989).
- [28] A. N. Antonov, I. S. Bonev, Chr. V. Christov, I. Zh. Petkov, *Nuovo Cimento* **A100**, 779 (1988).
- [29] K. Wildermuth, Y. C. Tang: *An Unified Theory of the Nucleus* (Academic Press, New York, 1977).

